A Five-Year Record of Summer Melt on Eurasian Arctic Ice Caps

MARTIN SHARP

Department of Earth and Atmospheric Sciences, University of Alberta, Edmonton, Alberta, Canada

LIBO WANG

Climate Research Division, Atmospheric Science and Technology Directorate, Environment Canada, Toronto, Ontario, Canada

(Manuscript received 14 January 2008, in final form 16 May 2008)

ABSTRACT

Climatologies and annual anomaly patterns (2000–04) of melt season duration and dates of melt onset/freeze-up on Eurasian Arctic ice masses were derived from Quick Scatterometer (QuikSCAT) backscatter data. Severnaya Zemlya, Russia, has later melt onset, earlier freeze-up, and shorter melt seasons than Svalbard, Norway/Novaya Zemlya, Russia. In all three archipelagos 2001 was the longest melt season and 2000 was the shortest. Anomalously long (short) melt seasons on Svalbard were associated with negative (positive) sea ice concentration anomalies along the north coast in June and August. Annual mean melt duration was strongly correlated with the mean (June + August) NCEP–NCAR reanalysis 850-hPa air temperature, allowing reconstruction of melt durations for the period of 1948–2005. The 2000–04 pentad had the second or third longest mean melt duration of all pentads in the 1950–2004 epoch, while the 1950–54 pentad probably had the longest. Integration of these results with previous results from Greenland and the Canadian Arctic identifies 2002 as the longest melt season in the 2000–04 period across the Arctic as a whole, and 2001 as the shortest. Correlation of melt duration anomalies for 19 discrete regions identifies seven spatially coherent areas of the Arctic with common patterns of variability in annual melt duration.

1. Introduction

Since the early 1990s there has been a sharp increase in the rate of global sea level rise, from a post-1961 average of 1.8 ± 0.5 mm yr^{-1} to a post 1993 average of 3.1 ± 0.7 mm yr^{-1} (Solomon et al. 2007). Recent estimates suggest that ocean warming accounts for about 1.6 ± 0.5 mm yr^{-1} of the post-1993 rate, and that wastage of small glaciers and ice caps accounts for about 60% of the remainder (Meier et al. 2007). The rate of glacier and ice cap wastage has increased recently as a result of more negative surface mass balances resulting from climate warming (Kaser et al. 2006), and probably also of increased rates of mass loss resulting from rapid retreat and thinning of tidewater glaciers (Meier et al. 2007).

Most regional-scale estimates of glacier surface mass balance either rely on extrapolations of field measurements made at a few generally small glaciers (Kaser et al. 2006), or are based on models that are in some way tuned to these observations (e.g., Zuo and Oerlemans 1997). This is especially true in the polar regions, where much of the glacier and ice cap area is found, but where long-term measurements of surface mass balance exist for only a handful of ice masses (Dyurgerov and Meier 2005). The extent to which these measurements are representative of regional-scale trends in surface mass balance is not well known. Thus, there is a clear need to develop more rigorous methods for upscaling the field measurements if we are to accurately assess the uncertainties associated with regional-scale mass balance estimates.

Because much of the interannual and longer-term variability in the surface mass balance of Arctic glaciers arises from variability in the summer balance [i.e., from rates of surface melt rather than rates of snow accumulation; see Koerner (2005) and Gardner and Sharp (2007)], knowledge of regional-scale patterns of summer melt and their temporal variability could form a basis for upscaling procedures. It will also help to iden-

Corresponding author address: Martin Sharp, Department of Earth & Atmospheric Sciences, 1-26 Earth Sciences Building, University of Alberta, Edmonton, AB T6G 2E3, Canada.
E-mail: martin.sharp@ualberta.ca

DOI: 10.1175/2008JCLI2425.1

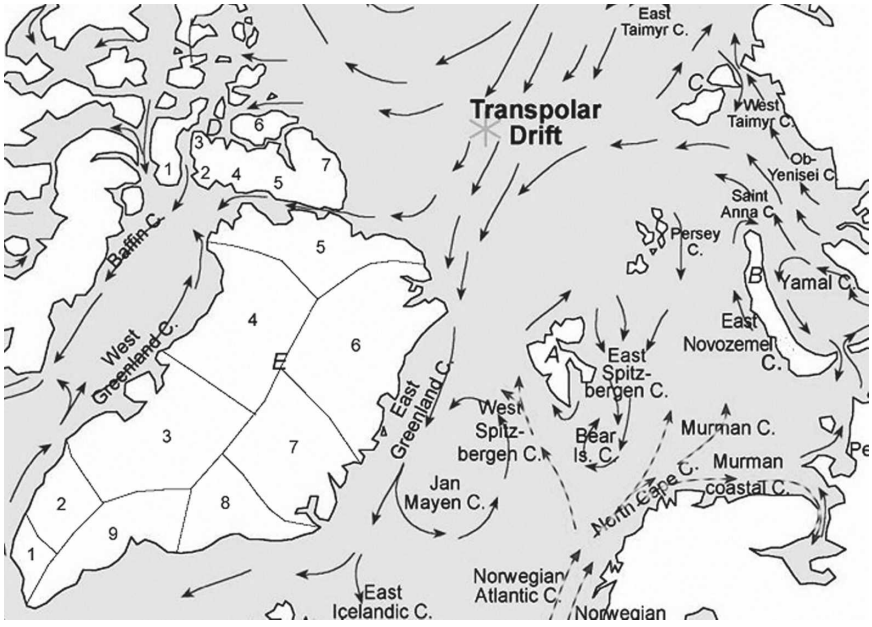

FIG. 1. Map of the Arctic showing the locations of Svalbard (A), Novaya Zemlya (B), Severnaya Zemlya (C), the Queen Elizabeth Islands (D), and Greenland (E) relative to the major Arctic Ocean current systems. Within Greenland, regions are numbered according to Wang et al. (2007). Within the Queen Elizabeth Islands, numbers refer to separate ice caps: Devon Island (1), Manson Icefield (2), Sydkap (3), Prince of Wales Icefield (4), Agassiz Ice Cap (5), Axel Heiberg Island (6), and Northern Ellesmere (7).

tify regions that are underrepresented in the global mass balance database.

The annual melt extent on the Greenland ice sheet has been mapped using satellite passive microwave data for the period since 1973 (Mote and Anderson 1995; Abdalati and Steffen 2001; Tedesco 2007; Mote 2007). However, melt extent is not a useful descriptor of summer melt on the smaller Arctic ice caps because almost all regions of these ice caps undergo melt every year. For these ice caps, the summer melt duration provides an alternative melt index that correlates well with the annual melting degree-day total on ice caps in the Canadian high Arctic (Wang et al. 2005) and on the Greenland ice sheet (Wang et al. 2007). While the coarse spatial resolution of satellite passive microwave data precludes their use for measuring this parameter over the smaller Arctic ice caps, enhanced resolution Ku-band scatterometer data from the Quick Scatterometer (QS) are well suited for this purpose (Wang et al. 2005, 2007).

Here we present measurements of summer melt duration on the major ice masses in the Eurasian Arctic archipelagos of Svalbard, Norway, and Novaya Zemlya and Severnaya Zemlya, Russia (Fig. 1; total ice-covered area = 78 500 km^2) for the 2000–04 period. We use these measurements to define climatological patterns of melt duration for each archipelago and compute annual anomalies from these patterns. We then investigate the principal geographical and climatological controls on both the mean summer melt duration in the Eurasian high Arctic and the annual anomaly patterns. This analysis complements previously published analyses for the same time period for Arctic Canada (Wang et al. 2005) and Greenland (Wang et al. 2007), providing a near-complete 5-yr snapshot of summer melt conditions on the major Arctic ice masses.

2. Methods

The basis for melt detection using QS data is the sharp reduction in microwave backscatter (measured by the normalized radar cross section, σ^0) that occurs when liquid water is present in the near-surface layers of snow and firn (Ulaby and Stiles 1981; Nghiem et al. 2001; Steffen et al. 2004; Wang et al. 2005, 2007; Ashcraft and Long 2006). Temporal variations in backscatter allow for the identification of the dates of melt onset and freeze-up in each grid cell, and of periods of refreezing during the melt season. This information allows for the calculation of melt duration.

The primary data source consists of enhanced resolution, slice-based (2.225-km gridcell spacing; effective

resolution ~5 km) backscatter images derived from the SeaWinds scatterometer on QS using the Scatterometer Image Reconstruction (SIR) algorithm (Early and Long, 2001; Long and Hicks 2005). We use descending pass images with horizontal polarization, which have effective measurement times of 1700–2100 LST for Svalbard, Severnaya Zemlya, and Novaya Zemlya.

Ice cap outlines were taken from the circum-Arctic map of permafrost and ground ice conditions dataset (Brown et al. 1998). To minimize mixed gridcell influences on the measured backscatter, only grid cells fully contained within the ice cap outlines were included in the study. Mixed grid cells were identified by overlaying the ice cap outlines on clear-sky images from the Moderate Resolution Imaging Spectroradiometer (MODIS) and were manually removed from the dataset. Grid cells in which bare glacier ice is exposed during the melt season were also removed from the dataset because freeze-up dates in these grid cells cannot be detected reliably (Wang et al. 2007). The proportions of the total ice covered areas included in the study were ~63% in Svalbard, 75% in Novaya Zemlya, and 84% in Severnaya Zemlya. Areas excluded from the study tend to be at relatively low elevations and are likely to have longer melt seasons on average than the areas included in the study. Thus, the results reported here are likely biased toward the higher-elevation regions of the larger ice masses in each region. The areas included in the study are the same for all years, however, so interannual comparisons are valid.

An empirical, gridcell-specific thresholding method was used to detect melt. For each grid cell, the mean winter backscatter (W_{mn}) was calculated from daily backscatter time series for the December–February period. Two melt thresholds were established as $M_1 = W_{mn} - a$, and $M_2 = W_{mn} - b$. All periods when either (i) σ^0 remained below M_1 for 3 or more consecutive days, or (ii) σ^0 dropped below M_2 for 1 day were categorized as melt days. In previous work, a and b were determined by tuning using air temperature measurements from on-ice weather stations to indicate when melt was occurring (Wang et al. 2007). Becacuse we did not have access to such measurements for this study, we used daily MODIS level 3 (V0004) 1-km-resolution land surface temperature (LST) products (cf. Hall et al. 2006, 2008) for tuning purposes. The errors in the MODIS products over snow are generally <1°C, and do not exceed 2°C (Wan et al. 2002). Given this uncertainty and the different timing of the QS and MODIS measurements, and the different temporal and spatial averaging involved in generation of the MODIS and QS products, we assumed that melt occurred on a given day if the MODIS LST was >−2°C. The choice of 3.5 and 5.0 dB as best estimates of a and b, respectively, resulted in the most consistent set of predictions of melt occurrence from the QS and MODIS datasets. These values are more stringent than those used by Ashcraft and Long (2006; 3 dB for a) and Wang et al. (2007; 2.0 and 3.0 dB for a and b, respectively) to detect melt on Greenland using QS data.

We used the MODIS LST products to generate estimates of the uncertainty associated with our QS-derived estimates of melt duration. Because the MODIS products can only be generated for clear-sky conditions, we counted the number of melting days derived using each dataset for days on which MODIS data were available. The MODIS overpass times for the study area are generally between 1100 and 1600 LST. For 20 test sites on Novaya Zemlya in 2000, 2001, and 2003, linear regression of QS melt duration (Q) against MODIS melt duration (M) gives $Q = 0.91M + 3.6$ days ($r^2 = 0.92$, $p < 0.001$, standard error of the estimate = 1.7 days). The comparison dataset included 60 data points with M ranging from 3 to 25 days. For 30 test sites on Svalbard from 2000 to 2003, where the dataset included 101 points and a range of M from 3 to 45 days, the relationship was $Q = 0.97M + 3.6$ days ($r^2 = 0.87$, $p < 0.001$, standard error of the estimate = 3.7 days). Thus, the QS estimates tend to be up to 3 days longer than the MODIS estimates over the calibration range. This is probably because QS can detect the presence of water in the subsurface even when the snow surface itself is frozen (Ashcraft and Long 2006). The standard errors of the melt duration estimates derived from regressing Q against M for Novaya Zemlya and Svalbard (1.7 and 3.7 days, respectively) are less than those derived from regressing Q and melt duration derived from on-ice air temperature measurements in Greenland (7.9 days; Wang et al. 2007) and the Canadian Arctic (10.1 days; Wang et al. 2005). This is likely because Q and M are both derived from measurements of properties of the snow surface.

3. Results

a. Melt climatologies

Five-year averages of the melt duration and dates of melt onset and freeze-up were computed for each grid cell and mapped for each of the three study regions (Fig. 2). Average melt durations are similar on Svalbard (60–110 days, mean = 77) and Novaya Zemlya (65–100 days, mean = 75), but are much shorter (30–75 days, mean = 51) on Severnaya Zemlya (Table 1). Melt typically begins between 20 May and 19 June on Svalbard, between 25 May and 14 June on Novaya Zemlya, and between 9 and 24 June on Severnaya Zemlya. Freeze-

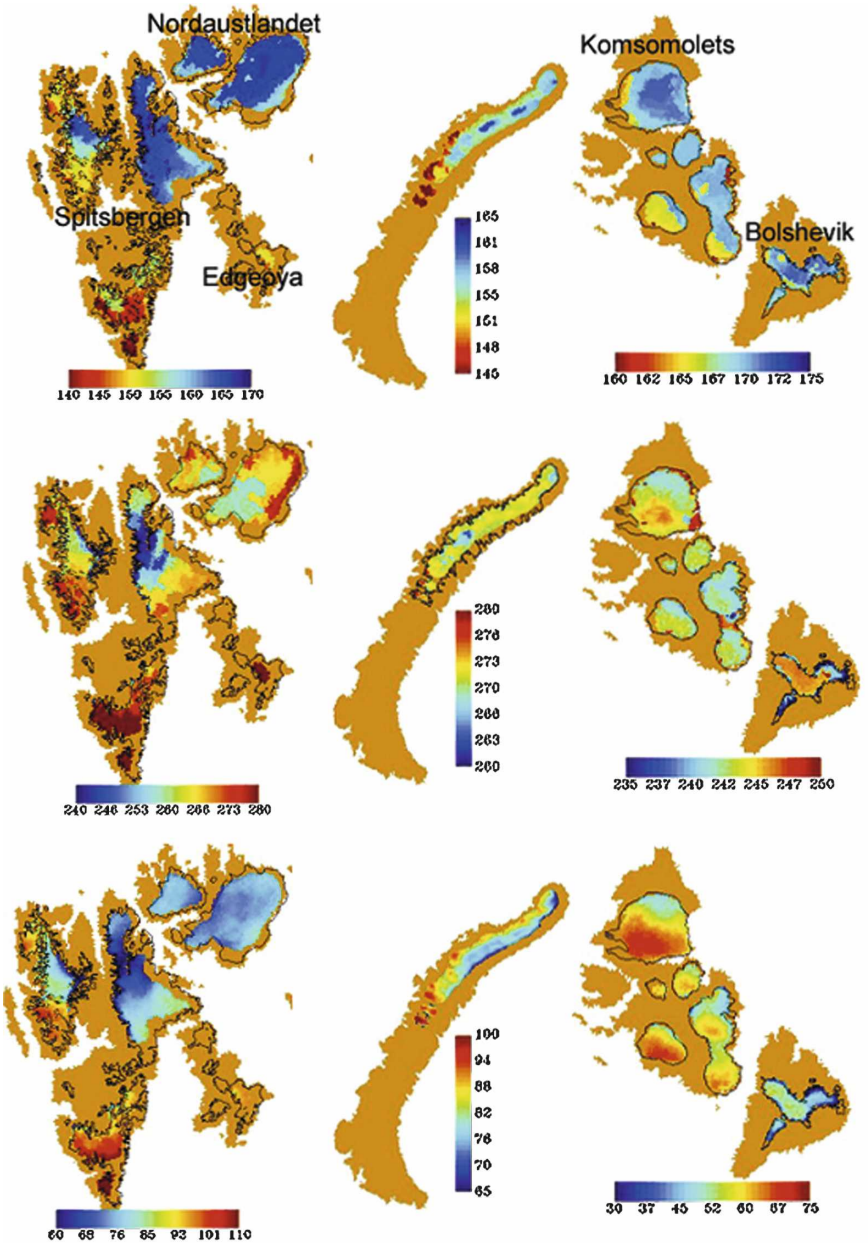

FIG. 2. The 2000–04 climatologies of (top) melt onset date (day of year), (middle) freeze-up date, and (bottom) melt duration (days) for (left) Svalbard, (middle) Novaya Zemlya, and (right) Severnaya Zemlya.

up usually occurs between 23 August and 7 September on Severnaya Zemlya, between 28 August and 7 October on Svalbard, and between 17 September and 7 October on Novaya Zemlya.

These patterns are consistent with the steep climatic gradient across the Eurasian High Arctic from relatively warmer, moister conditions on Svalbard in the west, to progressively colder and drier conditions with more prolonged seasonal sea ice cover farther east (Dowdeswell et al. 2002). Severnaya Zemlya generally lies within the climatological annual minimum sea ice extent for the period 1979–2000, while Novaya Zemlya lies between the annual minimum and maximum extents. On Svalbard, the north coast lies close to the annual minimum sea ice extent, the east coast lies between the annual maximum and the annual minimum, and the west coast lies close to open water year-round (Fetterer et al. 2002).

The major geographical controls on mean melt duration in each region were explored by regression

TABLE 1. Mean annual melt duration (days) (2000–04) in 19 regions of the Arctic, together with the 5-yr mean and standard deviation. For Greenland and the Queen Elizabeth Islands, the numbers in brackets refer to regions identified in Fig. 1. The mean elevation of each region is given in the final column. The area-weighted sum of annual melt duration anomalies for all regions (bottom row) is an index of annual melt duration for the whole Arctic.

Region	2000	2001	2002	2003	2004	Mean	Std dev	Mean elevation (m)
Svalbard	64.4	89.3	90.4	70.2	72.0	77.2	13.2	541
Novaya Zemlya	72.1	90.6	70.9	74.1	68.8	75.3	10.1	615
Severnaya Zemlya	46.5	52.6	52.9	56.7	45.4	50.8	6.3	505
Devon (1)	40.8	50.9	37.5	45.7	35.4	42.1	6.3	1080
Manson (2)	61.6	63.4	62.4	57.6	63.4	61.7	2.4	585
Sydkap (3)	49.0	49.2	32.7	44.1	45.1	44.0	6.7	827
Prince of Wales (4)	47.6	53.9	40.1	51.0	44.7	47.4	5.4	967
Agassiz (5)	29.8	32.6	16.2	29.8	22.9	26.3	6.7	1286
Axel Heiberg (6)	40.4	39.0	31.8	40.4	36.0	37.5	3.7	1073
North Ellesmere (7)	31.4	32.7	23.9	37.1	26.6	30.3	5.2	1171
South-southwest Greenland (1)	70.2	61.3	58.1	80.1	71.3	68.2	8.7	2035
Southwest Greenland (2)	45.5	33.7	35.2	45.7	49.5	41.9	7.1	2242
West Greenland (S) (3)	21.2	16.9	22.4	22.1	27.6	22.0	3.8	2359
West Greenland (N) (4)	12.4	13.6	16.8	16.7	15.4	15.0	1.9	2259
Northwest Greenland (5)	7.0	13.8	11.3	11.7	8.3	10.4	2.8	1817
Northeast Greenland (6)	4.9	4.4	17.0	7.6	6.1	8.0	5.2	2198
East Greenland (N) (7)	4.8	3.5	10.8	7.0	8.8	7.0	3.0	2840
East Greenland (S) (8)	16.1	9.2	22.7	17.8	20.9	17.3	5.2	2633
Southeast Greenland (9)	34.6	28.5	35.2	35.1	40.7	34.8	4.3	2283
Anomaly sum	−1.83	−2.60	2.46	0.89	1.14			

against the latitude, longitude, and elevation of each grid cell (Table 2). Surface elevations for each grid cell were obtained from a digital elevation model (DEM) derived from the Global 30 Arc-Second Elevation Data Set (GTOPO30) DEM that used the same grid as the QS data. All three variables are significant influences in each area. Latitude exerts the strongest influence on melt duration in Svalbard, while longitude is the most significant influence in Novaya Zemlya and Severnaya Zemlya. The negative correlation between longitude and melt duration in all three regions is consistent with the pattern of sea surface temperatures in the region, because all three areas are characterized by northward penetration of relatively warm waters along their western margins and southward penetration of colder waters along their eastern margins. The positive correlation between latitude and melt duration in Severnaya Zemlya reflects the fact that the most southeasterly island in the group (Bolshevik Island) is under the influence of southward-flowing cool waters, while the most northwesterly island (Komsomolets Island) is influenced by warmer northward-flowing waters. There is a clear northeast-to-southwest asymmetry in mean melt duration on the ice caps on Komsomolets Island that is absent from the ice caps on Bolshevik Island (Fig. 2). By contrast, on Novaya Zemlya, the melt season is longer on the northern flanks of the ice field than on the southern flanks because the northernmost flanks of the ice field lie on the warmer, western margin of the island.

Elevation is a more significant influence on melt duration in Svalbard ($r = -0.31$) than in the other two regions, probably because the range of elevations on Svalbard (1400 m) is appreciably larger than those on

TABLE 2. Results of regression analyses of mean annual melt duration (2000–04) against latitude, longitude, and elevation for Svalbard, Novaya Zemlya, and Severnaya Zemlya. Intercept and regression coefficients for latitude, longitude, and elevation are derived from multiple linear regression [as are multiple r^2 and significance level (p)]. Values of r^2 for single variables are derived from simple linear regression and are included to provide an indication of the relative importance of the different variables as influences on mean melt duration.

	Intercept	Latitude	Latitude (r^2)	Longitude	Longitude (r^2)	Elevation	Elevation (r^2)	Multiple r^2	p (MR)	n
Svalbard	822.5	−9.19	0.5	−0.33	0.11	−0.017	0.096	0.59	<0.001	4117
Novaya Zemlya	−114.7	4.2	0.14	−1.86	0.18	−0.0107	0.008	0.26	<0.001	3300
Severnaya Zemlya	816.5	−5.7	0.16	−3.14	0.49	0.0023	0.005	0.57	<0.001	2523

Novaya Zemlya (1068 m) and Severnaya Zemlya (956 m). In general, areas with relatively long melt seasons are characterized by both early melt onset and late freeze-up. The converse is true for areas with relatively short melt seasons. There are two major exceptions to this: Bolshevik Island in southeast Severnaya Zemlya and eastern Nordaustlandet in Svalbard, where the melt season both starts and ends late. In these areas, the late continuation of melt may reflect the fact that sea ice only disappears from the adjacent waters late in the melt season. Heat released from the newly open ocean may have the effect of prolonging the melt season in these areas.

b. Melt duration anomalies: Interannual differences

The anomalously long melt seasons during the 2000–04 period were 2001 (all areas), 2002 (Svalbard and Severnaya Zemlya), and 2003 (Novaya Zemlya and Severnaya Zemlya). Both 2000 and 2004 were relatively short seasons in all three areas (Table 1). Spatial patterns of melt duration anomalies in each year are shown in Fig. 3, and the results of multiple regression analyses of the relationships between annual melt duration anomalies in each region and latitude, longitude, and elevation are presented in Table 3. In 2001, positive anomalies occurred across the whole of Novaya Zemlya, in northern and eastern Svalbard, and northwest Severnaya Zemlya; 2002 was characterized by positive anomalies throughout Svalbard and in southeastern Severnaya Zemlya, and by quite strongly negative anomalies in Novaya Zemlya. In 2003, the anomalies were very positive in Severnaya Zemlya, weakly positive in northeast Novaya Zemlya, and strongly negative in northern and eastern Svalbard. In 2004, negative anomalies occurred across all three regions, while in 2000 they were concentrated in northern and eastern Svalbard, on Bolshevik Island in Severnaya Zemlya, and at higher elevations on Novaya Zemlya.

c. Variability in melt duration anomalies: Spatial patterns

The standard deviation of the melt duration in all grid cells for the period 2000–04 was 6.3 days on Severnaya Zemlya, 10.1 days on Novaya Zemlya, and 13.2 days on Svalbard. Thus, at the scale of whole archipelagos, variability in melt season length is greatest in the more maritime environment of Svalbard (Table 1). This may be a function of the regional sea ice regime. The largest melt duration anomalies (positive and negative) in Svalbard occur in the north. Sea ice retreated from the north coast in the positive anomaly years (2001 and 2002) but persisted there throughout the summer in the extreme negative anomaly year (2000; see Fetterer et al. 2002). Ice retreat from the coast would reduce the local albedo and open up an oceanic heat source that is absent in other years, accounting for the large variability in melt duration. In contrast, Severnaya Zemlya is more or less surrounded by sea ice in all months and this may suppress variability in melt duration by keeping albedo high and suppressing local oceanic heat sources. Here, the largest positive melt duration anomalies occurred in the southeast of the archipelago

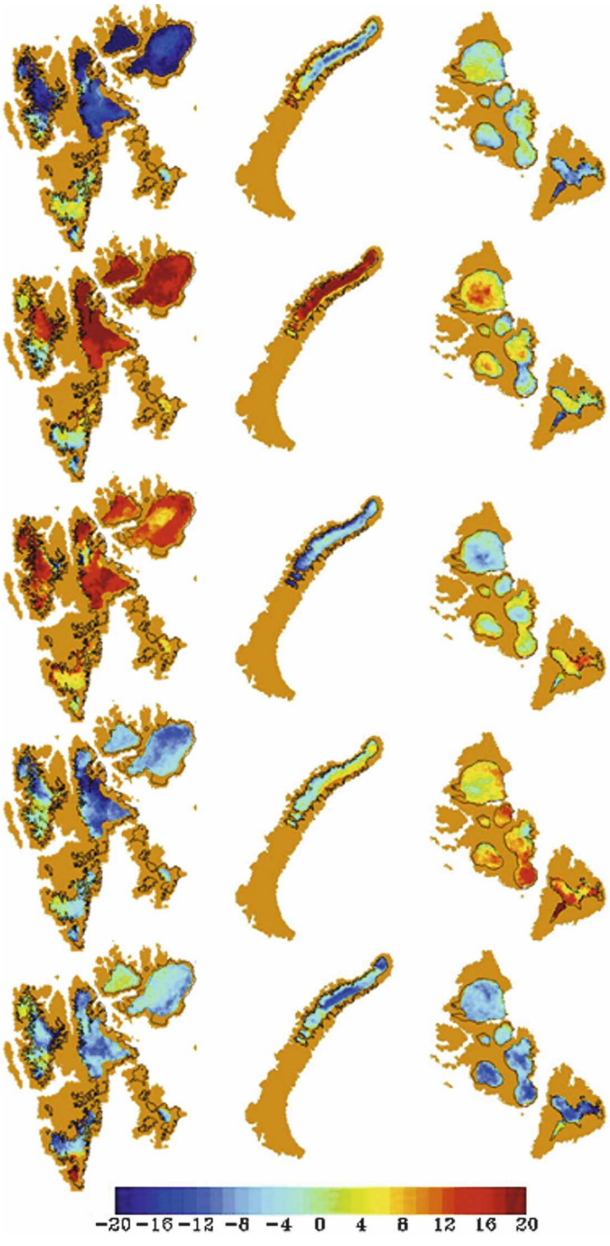

FIG. 3. Annual anomalies in melt duration (days) relative to the 2000–04 climatology for (left) Svalbard, (middle) Novaya Zemlya, and (right) Severnaya Zemlya. The top row is 2000 and the bottom row is 2004.

TABLE 3. Results of multiple regression analysis of the annual anomaly in melt season duration (relative to the 2000–04 climatology) against latitude, longitude, and elevation for Svalbard, Novaya Zemlya, and Severnaya Zemlya. All regressions are statistically significant at $p < 0.01$.

	2000	2001	2002	2003	2004
Svalbard					
Intercept (days)	610.3	−487.9	−214.3	94.0	−2.1
Latitude	−7.95	6.11	2.97	−1.16	0.02
Longitude	0.15	0.59	−0.37	−0.29	−0.08
Elevation	0.002	0.014	−0.002	−0.008	−0.006
r^2	0.64	0.55	0.13	0.18	0.05
Novaya Zemlya					
Intercept (days)	300.6	−954.6	−287.5	538.2	403.3
Latitude	−3.28	14.33	3.46	−8.88	−5.63
Longitude	−0.69	−1.99	0.17	2.13	0.38
Elevation	−0.020	0.015	0.012	0.005	−0.012
r^2	0.41	0.42	0.40	0.33	0.31
Severnaya Zemlya					
Intercept (days)	−173.8	−133.2	208.6	268.1	26.4
Latitude	2.42	2.37	−3.28	−3.40	−0.31
Longitude	−0.24	−0.61	0.56	0.13	−0.01
Elevation	0.004	0.012	−0.004	−0.004	−0.121
r^2	0.35	0.41	0.51	0.32	0.23

in 2002 and 2003, both of which are years when open water was present to the southeast of the archipelago in July (Fetterer et al. 2002).

Multiple regression of the standard deviation of the melt duration anomalies for each grid cell in each archipelago against latitude, longitude, and elevation shows that the variability of the anomalies (and hence melt duration) (i) increases with elevation in all 3 regions; (ii) increases with latitude in Svalbard and Novaya Zemlya, but decreases with increasing latitude in Severnaya Zemlya; and (iii) is greater in the west of Svalbard and Novaya Zemlya than in the east, while on Severnaya Zemlya it is greater in the east than in the west (Table 4). All of these relationships are statistically significant and in all cases the range of latitudes in each archipelago results in a larger range of standard deviations than does the range in longitude. The signs of the relationships between the standard deviation of melt duration anomalies and latitude, longitude, and elevation all imply that within-archipelago variability in melt duration is higher in areas with generally short mean melt season durations. This was confirmed for each region by simple linear regression, and is the opposite of what is observed at the regional scale.

TABLE 4. Results of multiple regression analysis of the relationships between the standard deviation of the annual melt duration anomalies in each grid cell and latitude, longitude, and elevation for Svalbard, Novaya Zemlya, and Severnaya Zemlya. All regressions are statistically significant at $p < 0.01$.

	Svalbard	Novaya Zemlya	Severnaya Zemlya
Intercept	−248.7	−167.0	136.1
Latitude	3.335	2.704	−1.721
Longitude	−0.090	−0.461	0.082
Elevation	0.002	0.004	0.001
r^2	0.46	0.13	0.42

A likely explanation for this result is that, because regions with shorter melt seasons have lower mean melt season air temperatures than regions with longer melt seasons, meteorological events that result in colder-than-normal conditions during the melt season probably reduce the length of the melt season in such regions more than they do in regions with higher mean temperatures. Detailed examination of backscatter time series for individual pixels confirms that the amplitude of backscatter response to summer cold periods tends to be much larger in pixels with short melt durations than in pixels with long melt durations. Thus, these cold periods are more likely to be excluded from the computation of melt duration in pixels where the melt duration is relatively short.

d. Melt duration: Climatic controls

Annual anomalies in the dates of melt onset and freeze-up were mapped for each region (Figs. 4 and 5) and annual averages were computed (Table 5). Anomalously early melt onset accounted for anomalously long melt seasons in 2002 (Svalbard) and 2001 and 2003 (Severnaya Zemlya), while late freeze-up was a factor in 2001 and 2003 (Severnaya Zemlya). Anomalously late melt onset contributed to short melt seasons in 2000 (Svalbard, Severnaya Zemlya), 2002 (Novaya

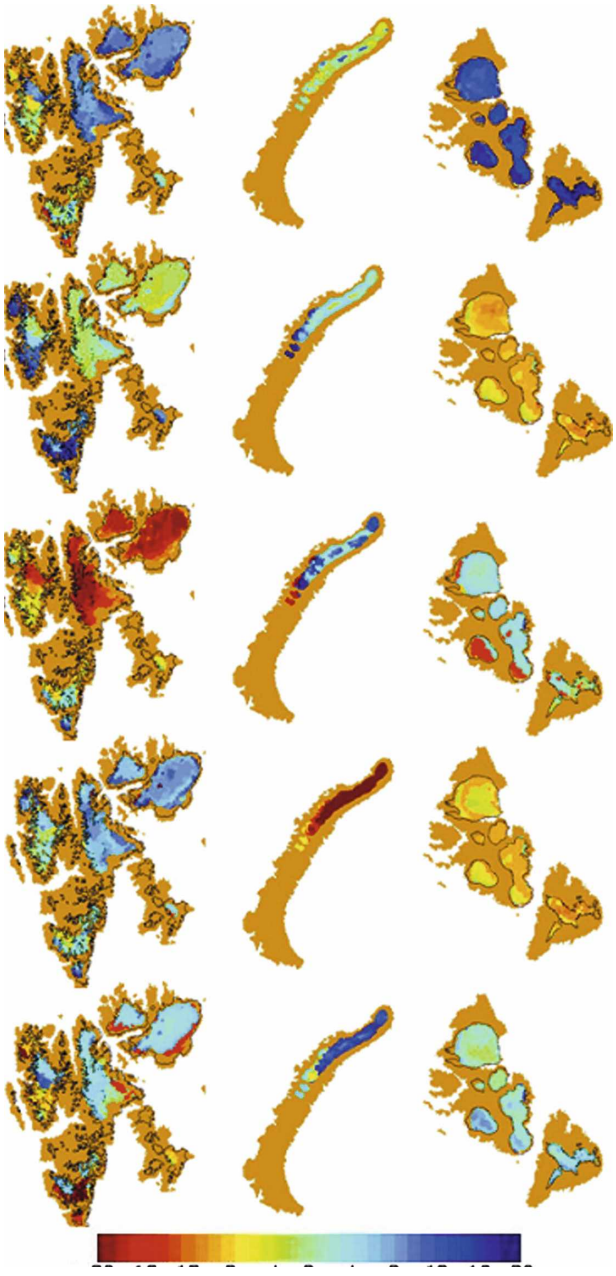

FIG. 4. Annual anomalies in melt onset date (day of year) relative to the 2000–04 climatology for (left) Svalbard, (middle) Novaya Zemlya, and (right) Severnaya Zemlya. The top row is 2000 and the bottom row is 2004.

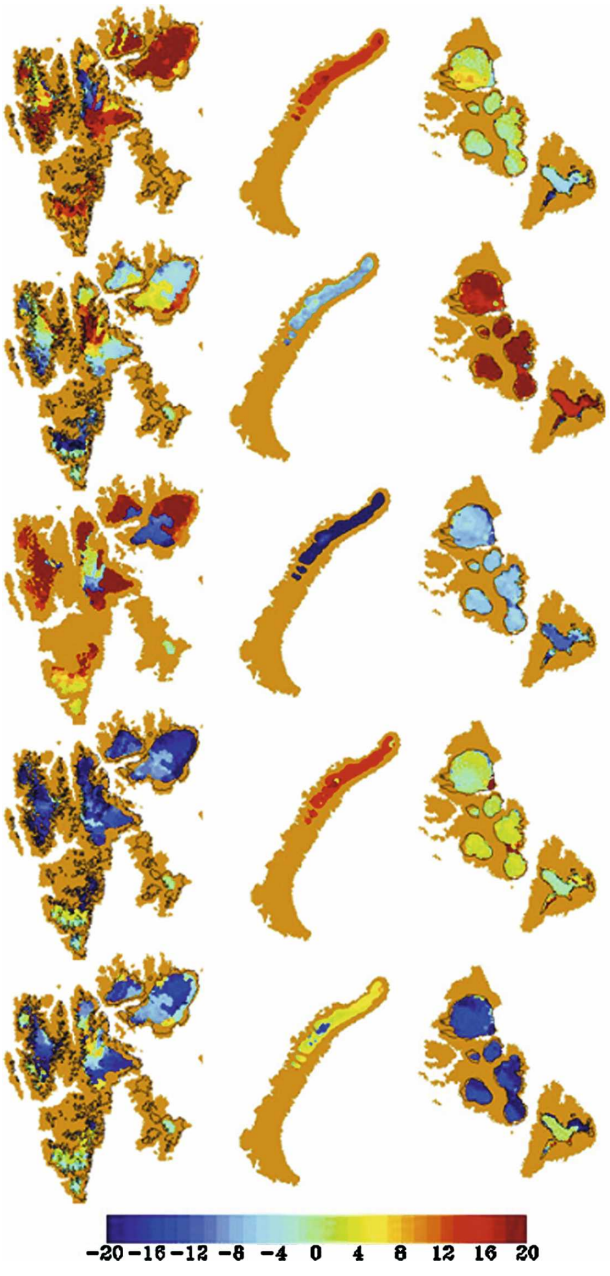

FIG. 5. Annual anomalies in freeze-up date (days) relative to the 2000–04 climatology for (left) Svalbard, (middle) Novaya Zemlya, and (right) Severnaya Zemlya. The top row is 2000 and the bottom row is 2004.

Zemlya), 2003 (Svalbard), and 2004 (Novaya Zemlya and Severnaya Zemlya), while early freeze-up was a factor in 2002 (Novaya Zemlya), 2003 (Svalbard), and 2004 (Svalbard and Severnaya Zemlya). Although 2001 was an anomalously long melt season on Novaya Zemlya, it was not associated with either early melt onset or late freeze-up. This is because there were fewer-than-normal prolonged periods of freeze-up within the 2001 melt season.

In previous work on the Canadian Arctic ice caps and the Greenland ice sheet, we found strong relationships between the melt duration and the July or summer-averaged geopotential height (at levels from 700 to 300 hPa) above the ice caps as determined from the National Centers for Environmental Prediction–National

TABLE 5. Annual anomalies in the dates of melt onset and freeze-up and in the length of the melt season for Svalbard, Novaya Zemlya, and Severnaya Zemlya for the period of 2000–04. Positive values imply late melt onset or freeze-up, and a long melt season, while negative values imply early melt onset or freeze-up and a short melt season. Average dates of melt onset and freeze-up and average melt durations for each region are also given for comparison.

Region		2000	2001	2002	2003	2004	Average onset (day of year)	Average freeze-up (day of year)	Average duration (days)
Svalbard	Anomaly onset	5.9	2.3	−12.5	5.5	−1.3	159.4	265.7	77.2
	Anomaly freeze-up	14.2	−0.0	−6.6	−13.8	−7.6			
	Anomaly length	−14.2	13.8	12.6	−7.1	−5.1			
Novaya Zemlya	Anomaly onset	−0.9	5.3	5.2	−19.1	9.5	153.8	271.3	75.3
	Anomaly freeze-up	14.3	−6.7	−24.5	14.1	2.7			
	Anomaly length	−1.9	16.8	−8.4	0.1	−6.6			
Severnaya Zemlya	Anomaly onset	13.9	−7.4	−0.0	−6.6	3.1	169.2	242.7	50.8
	Anomaly freeze-up	1.1	18.5	−6.6	3.1	−13.3			
	Anomaly length	−2.7	2.3	0.3	7.5	−7.4			

Center for Atmospheric Research (NCEP–NCAR) reanalysis (Kalnay et al. 1996). In this study, however, we found only weak and statistically insignificant relationships between these variables. By contrast, we found strong and statistically significant ($p < 0.05$) positive correlations ($r > 0.86$) between melt duration and the NCEP–NCAR air temperature at a geopotential height of 850 hPa in regions centered over each archipelago (Table 6). For all three regions, the strongest correlations were found with temperatures in June or the mean of June and August.

The slopes of the regression relationships between melt duration and mean (June + August) 850-hPa air temperature vary between the three regions (Table 7), being steepest in Svalbard (9.3 days $°C^{-1}$), and shallowest in Severnaya Zemlya (4.2 days $°C^{-1}$). This is consistent with the shapes of the mean annual temperature cycles at 850 hPa for the period of 1948–2005 in the three regions (Fig. 6). The average gradient in the monthly mean temperature over the periods on either side of the July temperature maximum is least for Svalbard in both the May–July (5°C $month^{-1}$) and July–September (−3°C $month^{-1}$) periods. It is similar for Novaya Zemlya (6.2°C $month^{-1}$) and Severnaya Zemlya (6.1°C $month^{-1}$) in the May–July period and steepest for Severnaya Zemlya (−3.8°C $month^{-1}$) in the July–September period. If the shape of the annual temperature cycle remains constant as the mean summer temperature changes, these differences in shape would result in the biggest changes in melt duration in Svalbard and the smallest changes in Severnaya Zemlya, as observed.

In Svalbard, the three longest melt seasons (2002, 2001, and 2004) were associated with negative sea ice concentration anomalies along the north coast of the archipelago in both June and August (and melt duration anomalies that became more positive with increasing latitude), while the two shortest melt seasons (2000 and 2003) had positive concentration anomalies in this region in both months [see Fetterer et al. (2002); and melt duration anomalies that became more negative with increasing latitude]. No consistent relationships between sea ice concentration anomalies and melt duration anomalies were apparent for either Novaya Zemlya or Severnaya Zemlya.

e. *Longer-term context*

To place the 5-yr study period in a longer-term context, we used the regression relationships between melt season duration and annual (June + August) mean 850-hPa air temperature over each region from the NCEP–NCAR Reanalysis (Table 7) to predict the annual melt

TABLE 6. Correlation coefficients between annual mean melt durations on glaciers and ice caps in Svalbard, Novaya Zemlya, and Severnaya Zemlya (2000–04) and mean air temperature for specific months at 850-hPa geopotential height in boxes centered over each region taken from the NCEP–NCAR reanalysis.

	June	July	August	September	June + July	June + August	June + September	July + August	July + September	August + September
Svalbard	0.94	0.00	0.82	−0.03	0.51	0.92	0.65	0.36	−0.02	0.45
Novaya Zemlya	0.86	−0.51	0.62	0.54	0.01	0.91	0.68	0.00	0.06	0.72
Severnaya Zemlya	0.93	−0.80	0.62	0.13	0.13	0.95	0.64	−0.22	−0.47	0.70

TABLE 7. Regression relationships between annual melt season duration and mean (June + August) 850-hPa air temperature in boxes centered over each region from the NCEP–NCAR reanalysis.

	Intercept (days)	Regression slope	r^2	Significance level
Svalbard	97.4	9.3	0.79	0.03
Novaya Zemlya	75.2	7.3	0.76	0.03
Severnaya Zemlya	59.3	4.2	0.88	0.01

duration for each year in the 1948–2005 period. Annual values were reexpressed as standardized anomalies from the 57-yr mean melt duration. The 5-yr (2000–04) average standardized anomaly was calculated for each region. In all cases the result was positive (Svalbard = 0.47, Novaya Zemlya = 0.52, and Severnaya Zemlya = 0.48), indicating that the study period was generally characterized by longer-than-average melt seasons. Although this approach incorrectly assumes no change in the ice surface area over the 1948–2005 period, we do not believe that this is a major source of error in the melt duration estimates because, as explained above, marginal areas of the ice masses are generally excluded from the analysis of melt durations.

If we consider all discrete 5-yr periods (pentads) between 1950 and 2004, the 2000–04 pentad has the second longest mean predicted melt duration on Novaya Zemlya (after 1950–54), and the third longest on Svalbard (after 1950–54 and 1970–74) and Severnaya Zemlya (after 1950–54 and 1955–59). Here, 2002 was predicted to be the second longest melt season since 1948 on Svalbard, 2001 the third longest on Novaya Zemlya, and 2003 the fourth longest on Severnaya Zemlya.

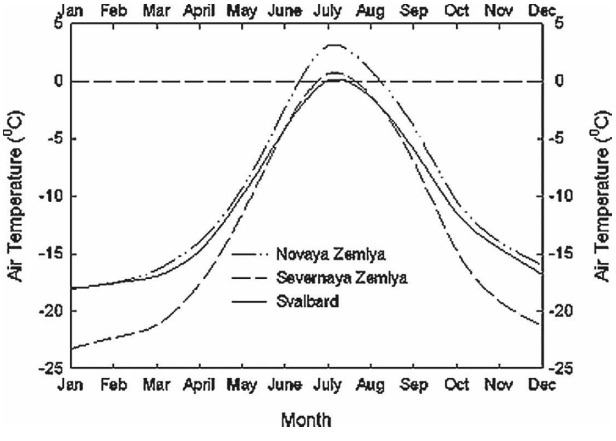

FIG. 6. Mean monthly air temperatures at the 850-hPa level for the period 1948–2005 in boxes centered over Svalbard, Novaya Zemlya, and Severnaya Zemlya, as derived from the NCEP–NCAR reanalysis.

Among the shorter summers, 2000 was the 51st longest melt season since 1948 on Svalbard, while 2002 was the 33rd longest on Novaya Zemlya, and 2004 the 45th longest on Severnaya Zemlya.

4. Discussion

a. Comparison with previous work

There have been few previous studies of the timing and duration of summer melt on the Eurasian Arctic ice caps. Smith et al. (2003) presented results for the timing of melt onset on five ice masses in Svalbard, Novaya Zemlya, and Severnaya Zemlya during the 1992–2000 period based on data from the European Remote Sensing (ERS) wind scatterometer. We compared their results with our results for the grid cells that were closest to the positions cited in their Table 1. Differences in the dates of mean, earliest, and latest melt onset ranged from 17 to 22 days, from 9 to 34 days, and from 20 to 34 days for Svalbard, Novaya Zemlya, and Severnaya Zemlya, respectively. In all cases our estimates of the dates of melt onset were earlier than theirs.

There are various possible explanations for this result. First, there is only 1 yr of overlap (2000) between the two studies, so the difference could indicate systematically earlier melt onset after 2000. This is consistent with average June 850-hPa temperatures over the three regions from the NCEP–NCAR reanalysis, which increased by 0.24°C (Svalbard), 0.33°C (Novaya Zemlya), and 0.43°C (Severnaya Zemlya) between 1992–2000 and 2000–04. However, regression analysis of the relationships between melt season duration and June 850-hPa temperatures over the three regions suggests sensitivities of between 3.24 days $°C^{-1}$ (Severnaya Zemlya) and 7.4 days $°C^{-1}$ (Svalbard), which would be insufficient to account for the observed differences in melt onset dates between this study and that of Smith et al. (2003).

Second, there are significant differences in the grid size of the two sets of measurements (25 km for ERS and 2.225 km for QS) and the timing of measurements relative to the diurnal melt cycle (1030 LST for ERS compared with 1700–2100 LST for QS). One might expect measurements made with the ERS scatterometer to be less sensitive to melt onset than those made with QS because of the lower spatial resolution of the ERS measurements and their early timing relative to the peak of the diurnal melt cycle.

Finally, and probably most significantly, the ERS wind scatterometer operates at a lower frequency (5.3 GHz) than QS (13.4 GHz), which means that its signal undergoes less absorption and penetrates deeper into wet snow than the QS signal, which makes it less sen-

sitive to the presence of water at the snow surface. Ashcraft and Long (2006) demonstrated that the ERS scatterometer detected melt onset over Greenland in 2000 systematically later than QS when threshold-based methods of melt detection were compared.

b. *Pan-Arctic perspective*

The completion of comparable analyses of summer melt duration on the Greenland ice sheet (nine regions; Wang et al. 2007) and the ice caps and larger glaciers of the three Eurasian Arctic archipelagos and Canada's Queen Elizabeth Islands (QEI; seven regions; Wang et al. 2005) makes it possible to discuss summer melt duration and its interannual variability across the entire Arctic. The mean melt duration (2000–04) was longer on Svalbard and Novaya Zemlya (>75 days) than anywhere else in the Arctic (Table 1). Among other Arctic regions, only south-southwest Greenland and the Manson Ice Field (QEI) had greater mean melt durations (>60 days) than Severnaya Zemlya (50.8 days). To derive an index of pan-Arctic summer melt duration, we summed the annual melt duration anomalies for the 19 regions (weighted by ice area) for each year (Table 1). For the entire Arctic land ice cover, the longest melt season was 2002, followed by 2004, 2003, 2000, and 2001. The area-weighted anomalies were negative in 2000 and 2001.

We examined monthly (JJA) maps of NCEP–NCAR 700-hPa temperature anomalies (relative to the 1979–2002 climatology) for the entire Arctic for each year and identified features that appear to explain the most significant melt duration anomalies for each year. The 700-hPa temperatures were examined for this analysis because the 700-hPa level is generally above the maximum surface height of all the major Arctic ice masses. In 2002, positive melt duration anomalies occurred in Svalbard (positive 700-hPa temperature anomalies all summer) and east and northeast Greenland (positive 700-hPa temperature anomalies in June and July), while negative anomalies occurred in Novaya Zemlya (negative 700-hPa temperature anomalies all summer), southwest and south-southwest Greenland (negative 700-hPa temperature anomalies in August), and throughout the QEI (negative 700-hPa temperature anomalies in July). In 2004, positive melt duration anomalies prevailed over much of Greenland, while there were negative anomalies in the Eurasian Arctic (negative 700-hPa temperature anomalies in August), the QEI, and northwest and northeast Greenland (negative 700-hPa temperature anomalies in June and July).

In 2003, melt duration anomalies were positive in Greenland (except for the northeast), Severnaya Zemlya, and the QEI (except for the Manson Ice Field, which has a very low mean elevation and lies mostly below 1000 m MSL), but strongly negative in Svalbard and Novaya Zemlya. Air temperatures at 700 hPa were unusually warm (relative to a 1979–2002 climatology) across Greenland and Severnaya Zemlya in June and August 2003, while in the QEI they were anomalously warm in July.

Most of Greenland and Severnaya Zemlya had negative melt duration anomalies in 2001, when June and July 700-hPa air temperature anomalies were negative over these regions. Positive anomalies were associated with positive 700-hPa air temperature anomalies throughout the summer over the QEI and northwest Greenland, and in June and August over Svalbard and Novaya Zemlya.

Here, 2000 was associated with negative melt duration anomalies across the Eurasian Arctic (negative 700-hPa temperature anomalies everywhere in June and July and over Svalbard in August) and Greenland (700-hPa temperature anomalies were negative in June and, in the north only, July and August). The exception to this was southwest and south-southwest Greenland, where melt duration anomalies were positive and 700-hPa temperature anomalies were positive in August.

Correlations between the 19 regional anomaly series allow identification of regionally coherent patterns of melt duration variability and teleconnections between geographically separate regions. In Greenland, there appear to be three spatially coherent groups (defined by interregional correlations $r > +0.8$): (i) southeast, south-southwest, southwest, and west Greenland (S; regions 1, 2, 3, and 9; Fig. 1), (ii) west Greenland (N), northeast Greenland, and east Greenland (N and S; regions 4, 6, 7, and 8; Fig. 1), and (iii) northwest Greenland (region 5; Fig. 1). The QEI ice caps (excluding Manson Ice Field) form another regionally coherent group, while the three Eurasian Arctic archipelagos are not well correlated with each other.

In terms of teleconnections, the annual melt duration anomalies in northwest Greenland are positively correlated ($r > +0.8$) with those in Severnaya Zemlya. The annual melt duration anomalies for the Devon, Sydkap, Prince of Wales, Agassiz, and Axel Heiberg Island ice caps are negatively correlated ($r < -0.8$) with those for northeast and east Greenland (N and S; regions 6, 7, 8; Fig. 1), and there are also negative correlations between the anomalies for the Devon ice cap and those for southeast Greenland and west Greenland (S; regions 3 and 9; Fig. 1). There are also negative correlations between the anomalies in Novaya Zemlya and southeast, west, and east Greenland (S; regions 3, 8 and 9; Fig. 1), and between Svalbard and southwest and

south-southwest Greenland (regions 1 and 2; Fig. 1). It should be emphasized that these apparent teleconnections are based upon only 5 yr of melt duration data and it remains to be seen whether they will prove to be robust features of longer time series.

5. Conclusions

Enhanced resolution data from the SeaWinds scatterometer on QS were used to map the timing of annual melt onset and freeze-up, and the duration of the summer melt season on the large glaciers and ice caps of Svalbard, Novaya Zemlya, and Severnaya Zemlya for the 2000–04 period. When combined with previously published results for the Canadian high Arctic (Wang et al. 2005) and Greenland (Wang et al. 2007), the results provide a comprehensive picture of summer melt conditions on land ice across the entire Arctic in the 2000–04 period. They also allow us to define the major spatial patterns in melt duration and their geographical controls, and to identify the nature, magnitude, and causes of interannual variability in melt duration within and between the three archipelagos. Because QS annual melt duration appears to be well correlated with the annual positive degree-day (PDD) total (Wang et al. 2005, 2007), this parameter provides a basis for estimating the distribution of PDD across the entire Arctic land ice cover. This distribution could be used to provide independent validation of downscaled temperature outputs from regional climate models, or as input to regional-scale temperature index melt models that could be used to compute the surface mass balance of glaciers and ice caps.

Consistent with large-scale gradients in summer climate across the Eurasian Arctic, the average melt duration is longest on Svalbard and shortest on Severnaya Zemlya. Annual melt begins first on Svalbard and last on Severnaya Zemlya, while freeze-up begins last on Novaya Zemlya. The average melt duration in each region is well correlated with latitude, longitude, and elevation. Melt seasons tend to be longer in the west of each region (reflecting the distribution of warm and cold ocean currents), in the south of Svalbard and Novaya Zemlya (but in the north of Severnaya Zemlya), and at lower elevations (although relationships with elevation are generally weak, probably because of the limited range of elevations found in this sector of the Arctic).

The predicted mean standardized melt duration anomaly in each region for the 2000–04 pentad was the second or third longest of all pentads in the 1950–2004 period. Five-year running mean standardized melt duration anomalies were generally $<+0.5$ from 1961 until 2000 and $>+0.5$ in the early to mid-1950s and after 1999. Within the 2000–04 period, the melt seasons 2001, 2002, and 2003 were generally longer than average, while those of 2000 and 2004 were relatively short. Interannual variability in the regionally averaged melt season duration was generally greatest in the relatively maritime environment of Svalbard and least in the more continental environment of Severnaya Zemlya. Within archipelagos, however, regions with shorter melt seasons generally displayed greater interannual variability in melt duration. Interannual variability in the mean annual melt duration for each archipelago was positively correlated with the mean (June + August) 850-hPa air temperature derived from the NCEP–NCAR reanalysis. This suggests that, in the Eurasian Arctic, changes in the timing of melt onset and freeze-up (rather than in the magnitude of peak summer temperatures) are the primary control on summer melt duration. Anomalously long (short) melt seasons on Svalbard were also associated with negative (positive) sea ice concentration anomalies along the north coast of the archipelago in both June and August. No obvious relationships between annual melt duration and sea ice concentration were apparent for either Novaya Zemlya or Severnaya Zemlya.

The results from this analysis were combined with those from previous similar analyses of melt duration in the Canadian high Arctic and on the Greenland ice sheet. For the Arctic as a whole, the sum of area-weighted melt duration anomalies identifies 2002 as the longest melt season in the 2000–04 pentad and 2001 as the shortest. In 2002, positive melt duration anomalies were recorded in Svalbard, Severnaya Zemlya, and all of Greenland except for the southwestern part. In 2001, negative anomalies occurred throughout Greenland except for the northwest, while positive anomalies were characteristic of the Eurasian and Canadian Arctic. Thus, the sign of melt duration anomalies in Greenland tends to dominate the pan-Arctic pattern.

Correlation analysis of regionally averaged patterns of interannual melt duration variability reveals essentially independent patterns of variation in the Canadian high Arctic, Svalbard, Novaya Zemlya, Severnaya Zemlya, and in three distinct regions of Greenland—(i) southeast, south-southwest, southwest, and west Greenland (S; regions 1, 2, 3, and 9; Fig. 1), (ii) west Greenland (N), northeast Greenland, and east Greenland (N and S; regions 4, 6, 7 and 8; Fig. 1), and (iii) northwest Greenland (region 5; Fig. 1). There is limited evidence for teleconnections between regions. For instance, there are positive correlations between patterns of melt duration variability in northwest Greenland and Severnaya Zemlya, and negative correlations between (i) the

Canadian high Arctic and northeast and east Greenland, (ii) Novaya Zemlya and southeast, west, and east Greenland (S), and (iii) Svalbard and southwest and south-southwest Greenland. The database from which these teleconnections are identified is, however, relatively limited and longer time series are required to confirm whether or not they are real.

Acknowledgments. Funded by the Canadian Foundation for Climate and Atmospheric Sciences through the Polar Climate Stability Network, Environment Canada through the CRYSYS program, and NSERC (Canada). We thank David Long for assistance with obtaining the QuikSCAT data, Zhengming Wan for assistance with the MODIS LST data, Gabriel Wolken for comments on an earlier draft, and Barry Goodison for his encouragement of this work. We also acknowledge helpful reviews by three anonymous referees.

REFERENCES

Abdalati, W., and K. Steffen, 2001: Greenland ice sheet melt extent: 1979-1999. *J. Geophys. Res.,* **106,** 33 983–33 988.

Ashcraft, I. S., and D. G. Long, 2006: Comparison of methods for melt detection over Greenland using active and passive microwave measurements. *Int. J. Remote Sens.,* **27,** 2469–2488.

Brown, J., O. J. Ferrians Jr., J. A. Heginbottom, and E. S. Melnikov, 1998: Circum-Arctic map of permafrost and ground ice conditions. National Snow and Ice Data Center/World Data Center for Glaciology, Denver, CO, digital media. [Available online at http://nsidc.org/data/ggd318.html; updated 2001.]

Dowdeswell, J. A., and Coauthors, 2002: Form and flow of the Academy of Sciences Ice Cap, Severnaya Zemlya, Russian High Arctic. *J. Geophys. Res.,* **107,** 2076, doi:10.1029/2000JB000129.

Dyurgerov, M. B., and M. F. Meier, 2005: Glaciers and the changing earth system: A 2004 snapshot. INSTAAR, University of Colorado Occasional Paper 58, 117 pp.

Early, D. S., and D. G. Long, 2001: Image reconstruction and enhanced resolution imaging from irregular samples. *IEEE Trans. Geosci. Remote Sens.,* **39,** 291–302.

Fetterer, F., K. Knowles, W. Meier, and M. Savoie, 2002: Sea ice index. National Snow and Ice Data Center, Boulder, CO, digital media. [Available online at http://nsidc.org/data/seaice_index/; updated 2007.]

Gardner, A. S., and M. Sharp, 2007: Influence of the Arctic circumpolar vortex on the mass balance of Canadian high Arctic glaciers. *J. Climate,* **20,** 4586–4598.

Hall, D. K., R. S. Williams Jr., K. A. Casey, N. E. DiGirolamo, and Z. Wan, 2006: Satellite-derived, melt-season surface temperature of the Greenland Ice Sheet (2000–2005) and its relationship to mass balance. *Geophys. Res. Lett.,* **33,** L11501, doi:10.1029/2006GL026444.

——, ——, S. B. Luthcke, and N. E. DiGirolamo, 2008: Greenland ice sheet surface temperature, melt and mass loss: 2000-06. *J. Glaciol.,* **54,** 81–93.

Kalnay, E., and Coauthors, 1996: The NCEP/NCAR 40-Year Reanalysis Project. *Bull. Amer. Meteor. Soc.,* **77,** 437–471.

Kaser, G., J. G. Cogley, M. B. Dyurgerov, M. F. Meier, and A. Ohmura, 2006: Mass balance of glaciers and ice caps: Consensus estimates for 1961–2004. *Geophys. Res. Lett.,* **33,** L19501, doi:10.1029/2006GL027511.

Koerner, R. M., 2005: Mass balance of glaciers in the Queen Elizabeth Islands, Nunavut, Canada. *Ann. Glaciol.,* **42,** 417–423.

Long, D. G., and B. R. Hicks, 2005: Standard BYU QuikSCAT/SeaWinds land/ice image products. Brigham Young University, MERS Tech. Rep. MERS 05-04 and ECEN Department Rep. TR-L130-05.04, 30 pp.

Meier, M. F., M. B. Dyurgerov, U. K. Rick, S. O'Neel, W. T. Pfeffer, R. S. Anderson, S. P. Anderson, and A. F. Glazovsky, 2007: Glaciers dominate eustatic sea level rise in the 21st century. *Science,* **317,** 1064–1067.

Mote, T. L., 2007: Greenland surface melt trends 1973–2007: Evidence of a large increase in 2007. *Geophys. Res. Lett.,* **34,** L22507, doi:10.1029/2007GL031976.

——, and M. R. Anderson, 1995: Variations in snowpack melt on the Greenland ice sheet based on passive-microwave measurements. *J. Glaciol.,* **41,** 51–60.

Nghiem, S. V., K. Steffen, R. Kwok, and W. Y. Tsai, 2001: Detection of snowmelt regions on the Greenland ice sheet using diurnal backscatter change. *J. Glaciol.,* **47,** 539–547.

Smith, L. C., Y. Sheng, R. R. Forster, K. Steffen, K. E. Frey, and D. E. Alsdorf, 2003: Melting of small Arctic ice caps observed from ERS scatterometer time series. *Geophys. Res. Lett.,* **30,** 2034, doi:10.1029/2003GL017641.

Solomon, S., D. Qin, M. Manning, Z. Chen, M. Marquis, K. B. Averyt, M. Tignor, and H. L. Miller, Eds., 2007: *Climate Change 2007: The Physical Science Basis.* Cambridge University Press, 996 pp.

Steffen, K., S. V. Nghiem, R. Huff, and G. Neumann, 2004: The melt anomaly of 2002 on the Greenland Ice Sheet from active and passive microwave satellite observations. *Geophys. Res. Lett.,* **31,** L20402, doi:10.1029/2004GL020444.

Tedesco, M., 2007: Snowmelt detection over the Greenland ice sheet from SSM/I brightness temperature daily variations. *Geophys. Res. Lett.,* **34,** L02504, doi:10.1029/2006GL028466.

Ulaby, F. T., and W. H. Stiles, 1981: Microwave response of snow. *Adv. Space Res.,* **1,** 131–149.

Wan, Z., Y. Zhang, Q. Zhang, and Z.-L. Li, 2002: Validation of the land surface temperature products retrieved from Terra Moderate Resolution Imaging Spectroradiometer data. *Remote Sens. Environ.,* **83,** 163–180.

Wang, L., M. J. Sharp, B. Rivard, S. Marshall, and D. Burgess, 2005: Melt season duration on Canadian Arctic ice caps, 2000–2004. *Geophys. Res. Lett.,* **32,** L19502, doi:10.1029/2005GL023962.

——, ——, ——, and K. Steffen, 2007: Melt season duration and ice layer formation on the Greenland ice sheet, 2000–2004. *J. Geophys. Res.,* **112,** F04013, doi:10.1029/2007JF000760.

Zuo, Z., and J. Oerlemans, 1997: Contribution of glacier melt to sea-level rise since AD 1865: A regionally differentiated calculation. *Climate Dyn.,* **13,** 835–845.